Available online at www.sciencedirect.com
ScienceDirect
Journal of Nuclear Materials 367–370 (2007) 806–811
journal of nuclear materials
www.elsevier.com/locate/jnucmat

Accumulation of helium in tungsten irradiated by helium and neutrons

Q. Xu [a,*], N. Yoshida [b], T. Yoshiie [a]

[a] Research Reactor Institute, Kyoto University, Noda, Kumatori-cho, Sennan-gun, Osaka 590-0494, Japan
[b] Research Institute for Applied Mechanics, Kyushu University, Fukuoka 816-8580, Japan

Abstract

Effects of helium on the microstructural evolution in tungsten were investigated using computer simulation based on a rate theory. Two cases were considered: helium with high energy (1 keV) and low flux (10^{18}/m^{2}s) and helium with low energy (30 eV, which cannot produce displacement damage) and high flux (10^{22}/m^{2}s). Neutron irradiation at 10^{-6} dpa/s and 873 K was used in the calculations as a typical irradiation condition. Helium–vacancy clusters with high concentration were formed near the incident surface during neutron and helium irradiations. The formation of helium–vacancy clusters suppressed the helium diffusion deeper into the specimen. The results show that a helium plasma with low energy and high flux has a greater effect on the accumulation of helium–vacancy clusters near the incident surface than would a helium plasma with high energy and low flux.

1. Introduction

Plasma-facing materials (PFMs) in a fusion reactor suffer two types of damage: displacement damage caused by high energy neutrons, and surface damage, such as erosion, sputtering and blistering, caused by hydrogen and helium from the plasma. Although these types of damage occur simultaneously, usually, they are investigated individually. The effects of helium ion irradiation on high-Z materials, which are potential candidates for the armor materials of the plasma-facing components, have been studied [1–4]. In these studies, blistering, erosion and microstructural evolution were examined. Helium, which has a strong interaction with vacancies [5,6], forms a high density of helium bubbles and leads to blistering at the incident surface. In addition, some experimental results showed that mechanical properties of tungsten influenced even under irradiation using 8-keV helium ions [3], where the damage peak was about 10 nm, and the helium existed at a depth of more than 140 nm from the surface [4]. These results suggest that injected helium interacts with lattice defects produced by the neutron irradiation in the fusion reactor. Recent simulation results based on a simple model using rate theory, where the diffusion of helium and the point defects produced by neutron irradiation were considered, agreed with the suggestion and indicated that helium was trapped by vacancies to form

* Corresponding author. Tel.: +81 724 51 2417; fax: +81 724 51 2620.
E-mail address: xu@rri.kyoto-u.ac.jp (Q. Xu).

0022-3115/$ - see front matter © 2007 Elsevier B.V. All rights reserved.
doi:10.1016/j.jnucmat.2007.03.078

helium–vacancy clusters in tungsten even in the region deeper than the range of helium [7]. In order to gain a better understanding of the performance of tungsten under the ITER condition, in the present work, we focused on the damage evolution in tungsten with simultaneous irradiation by helium and neutrons. In the case of ITER, the peak particle flux is estimated to be $10^{21}/m^2s$ at the first wall and $10^{24}/m^2s$ at the divertor, respectively [8]. The expected average energy is several keV at the first wall and 0.5 keV at the divertor.

2. Outline of the model

The damage due to neutron irradiation and the effect of helium originating from the plasma were considered simultaneously in the present simulation of microstructural evolution. Helium with high energy (1 keV) and low flux ($10^{18}/m^2s$), and with low energy (30 eV) and high flux ($10^{22}/m^2s$) were taken as typical cases for the first wall and the divertor, respectively. In the case of 1 keV-helium irradiation, defect production by the helium is taken into account, which is different from the model used in Ref. [7], but there are no displacement events for the 30 eV-helium irradiation. In contrast to the uniform damage produced by neutron irradiation, injected helium and associated damage is located close to the incident surface. In the present model, the depth distributions are simply assumed to be rectangular shape based on calculations using TRIM code [9], where the threshold displacement energy in tungsten was assumed to be 50 eV, which depends strongly on orientation [10]. Helium, interstitials, and vacancies could migrate freely in the matrix, and their concentrations at both surfaces were zero at any time. The time evolution of the concentration of point defects, defect clusters and helium were calculated using dynamic rate theory with the following assumptions:

(1) Only helium, interstitials, and vacancies are mobile.
(2) Maximum number of helium atoms absorbed by a vacancy is six.
(3) Clusters of a vacancy and n He atoms (nHe–V) cannot absorb an interstitial if $n \geqslant 4$.
(4) Thermal dissociation is only considered for helium–interstitial clusters.
(5) The rate of interstitial type dislocation loops formed directly by the cascade is assumed to be 0.1% of the defect production rate according to the PKA (primary knock-on atom) energy spectrum analysis [11].

In addition, the formation of vacancy clusters is neglected in the present study to simplify the modeling, since the mobility of vacancy is relatively low for the present conditions.

Throughout this paper, the concentrations are given in fractional units. The rate of concentration change of interstitials, vacancies, helium and helium–vacancy clusters can be expressed as

$$\begin{aligned}\frac{dC_i}{dt} &= 0.999(P + P_{D\text{–}He}(x)) + D_i\frac{\partial^2 C_i}{\partial x^2} \\ &\quad - Z_{iHe}(M_i + M_{He})C_iC_{He} - Z_{iv}M_iC_iC_v \\ &\quad - 2Z_{ii}M_iC_i^2 - Z_{Li}M_i(C_{Li}C_L)^{1/2}C_i - Z_{Si}M_iC_SC_i \\ &\quad - Z_{Hei}M_iC_i(C_{Hev} + C_{2Hev} + C_{3Hev}),\end{aligned} \tag{1}$$

$$\begin{aligned}\frac{dC_v}{dt} &= P + P_{D\text{–}He}(x) + D_v\frac{\partial^2 C_v}{\partial x^2} - Z_{iHe}(M_v + M_{He})C_vC_{He} \\ &\quad - Z_{iv}M_iC_iC_v - Z_{vHei}M_vC_{Hei}C_v \\ &\quad - Z_{Lv}M_v(C_{Li}C_L)^{1/2}C_v - Z_{Sv}M_vC_SC_v,\end{aligned} \tag{2}$$

$$\begin{aligned}\frac{dC_{He}}{dt} &= P_{He}(x) + D_{He}\frac{\partial^2 C_{He}}{\partial x^2} - Z_{iHe}(M_i + M_{He})C_iC_{He} \\ &\quad - Z_{vHe}(M_v + M_{He})C_vC_{He} \\ &\quad - Z_{Hev}M_{He}C_{He}(C_{Hev} + C_{2Hev} \\ &\quad + C_{3Hev} + C_{4Hev} + C_{5Hev}) \\ &\quad - Z_{LHe}M_{He}(C_{Li}C_L)^{1/2}C_{He} - Z_{SHe}M_{He}C_SC_{He} \\ &\quad + Z_{Hei}M_iC_i(C_{Hev} + 2C_{2Hev} + 3C_{3Hev}) \\ &\quad + Z_{vHei}M_vC_{Hei}C_v + EMIT_{Hei}C_{Hei},\end{aligned} \tag{3}$$

$$\begin{aligned}\frac{dC_{Hei}}{dt} &= Z_{iHe}(M_i + M_{He})C_iC_{He} - Z_{vHei}M_vC_{Hei}C_v \\ &\quad - EMIT_{Hei}C_{Hei},\end{aligned} \tag{4}$$

$$\begin{aligned}\frac{dC_{2Hev}}{dt} &= Z_{Hev}M_{He}C_{He}C_{Hev} - Z_{Hev}M_iC_iC_{2Hev} \\ &\quad - Z_{Hev}M_{He}C_{He}C_{2Hev},\end{aligned} \tag{5}$$

$$\frac{dC_{4Hev}}{dt} = Z_{Hev}M_{He}C_{He}C_{3Hev} - Z_{Hev}M_{He}C_{He}C_{4Hev}, \tag{6}$$

$$\frac{dC_{6Hev}}{dt} = Z_{Hev}M_{He}C_{He}C_{5Hev}, \tag{7}$$

where P and $P_{D\text{–}He}$ are the production rate of Frenkel pairs by neutron and helium irradiations, respectively. D is the diffusion coefficient of point defects or helium. M_i, M_v and M_{He} are the mobility of interstitials, vacancies and helium, respectively, which is related to the migration activation energy E_m by $v\exp(-E_m/kT)$, where v is the jump frequency. The values of D are equal to a^2M, where a is one atomic distance. Z is the site numbers of

the spontaneous reaction of each process. Details of the equation were described in Ref. [7].

$P_{\text{D–He}}$ and P_{He} in Eqs. (1)–(3) were the defect production rate and injection rate of helium, respectively, which is only produced close to the incident surface. They are expressed as

$$\begin{aligned} &P_{\text{D–He}}(x) = p_{\text{D–He}}, \quad P_{\text{He}}(x) = p_{\text{He}} \\ &\quad 0.1\ \text{nm} < x < 0.3\ \text{nm for 30 eV} \\ &\quad \text{and } 1\ \text{nm} < x < 3\ \text{nm for 1 keV}, \\ &P_{\text{D–He}}(x) = 0, \quad P_{\text{He}}(x) = 0 \\ &\quad x < 0.1\ \text{nm}, \text{or } x > 0.3\ \text{nm for 30 eV} \\ &\quad \text{and } x < 1\ \text{nm}, \text{or } x > 3\ \text{nm for 1 keV}. \end{aligned} \tag{8}$$

The rate of concentration change of interstitial loops C_{L} and interstitials aggregated in the loops C_{Li} in Eq. (1) can be expressed as

$$\frac{dC_{\text{L}}}{dt} = Z_{\text{ii}} M_{\text{i}} C_{\text{i}}^2 + 0.001(P + P_{\text{D–He}}(x)), \tag{9}$$

$$\frac{dC_{\text{Li}}}{dt} = Z_{\text{Li}} M_{\text{i}} (C_{\text{Li}} C_{\text{L}})^{1/2} C_{\text{i}} - Z_{\text{Lv}} M_{\text{v}} (C_{\text{Li}} C_{\text{L}})^{1/2} C_{\text{v}}. \tag{10}$$

Eqs. (5)–(7) express the time dependence of concentration of helium–vacancy clusters. The parameters used in the present simulations are listed in Table 1, where we assumed the interstitial migration energy to be 0.15 eV [13] which is higher than the value 0.054 eV obtained by Dausinger [14], since the purity of tungsten used in the fusion reactor will be low. There are few data on the dissociation energy of helium–interstitial pairs; it was assumed to be 0.5 eV instead of 1.93 eV, which was the dissociation energy of a helium atom from a dislocation [15].

Table 1
Parameters used in simulations

P (s^{-1})	10^{-6}
$p_{\text{D–He}}$ (s^{-1})	4×10^{-3} for 1 keV
$p_{\text{D–He}}$ (s^{-1})	0 for 30 eV
p_{He} (s^{-1})	8×10^{-3} for 1 keV
p_{He} (s^{-1})	2.4×10^{2} for 30 eV
E_{m}^{i} (eV)	0.15 eV
E_{m}^{V} (eV)	1.4 eV [12]
E_{m}^{He} (eV)	0.3 eV [12]
$E_{\text{EMIT (He–i)}}$ (eV)	0.5 eV
C_{S}	10^{-10}
Z	1
ν (s^{-1})	10^{13}

To maintain calculation accuracy and decrease calculation time, the thickness of the sample was selected to be about 0.067 mm; this is roughly the thickness of a typical transmission electron microscopy sample.

3. Results and discussion

3.1. Damage accumulation at the first wall surface

The effects of a helium plasma with energy 1 keV and flux $10^{18}/m^2s$ on the formation of helium–vacancy clusters were studied. Fig. 1(a) shows the time and depth dependence of helium concentration in 0.067 mm thick tungsten at 873 K, without any damage produced by helium and neutron irradiations. In this case, the concentration of helium

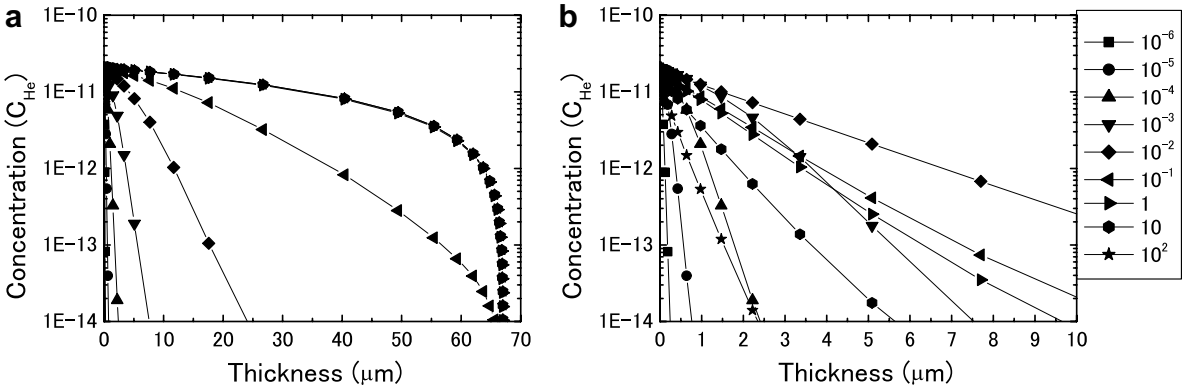

Fig. 1. Time and depth dependence of helium concentration in tungsten at 873 K with energy of 1 keV and flux of $10^{18}/m^2s$ without damage produced by helium and neutron irradiation (a), and with damage produced by helium and neutron irradiations (b). Irradiation times for each curve, in seconds, are shown in the insert legend.

increased with increasing time (except near the incident surface) and decreased with increasing depth, and the distribution of helium saturated at a concentration near 10^{-11} after 1 s. Fig. 1(b) shows the time and depth dependence of helium concentration when damage production by helium and neutron irradiations is included. With elapsed irradiation time to 0.01 s, the sample internal helium concentration increased first, and then decreased with increasing irradiation time. The highest concentration of helium, near the incident surface, was the same as that shown in Fig. 1(a). The decrease in helium concentration with increasing irradiation time after 0.01 s suggests that the most of the injected helium is trapped by the radiation induced defects and thus diffusion of helium to the deeper part of the specimen decreased.

Fig. 2 shows the depth distribution of helium–vacancy clusters, i.e., He–V (a) and 6 He–V (b) clusters, for several irradiation times. Time and depth dependence of formation of the helium–vacancy clusters 2 He–V, 3 He–V, 4 He–V and 5 He–V are the same as He–V. The concentrations of He–V and 6 He–V clusters decreased drastically near the incident surface in a region 0.05 μm thick after irradiation of 1 s. He–V and 6 He–V clusters with high concentration were formed in this narrow region, and their concentrations increased with increasing irradiation time. In order to investigate the reason of formation of He–V clusters with high concentration, the effects of helium only irradiation on the formation of helium–vacancy clusters were investigated. It was clear that the formation of He–V and 6 He–V clusters near the incident surface were caused by helium only irradiation. The concentration of 6 He–V clusters was two orders of magnitude higher than that of He–V clusters after irradiation of 10^2 s. He–V and 6 He–V clusters were also formed in the region deeper than 0.05 μm, which was caused by neutron irradiation, although their concentrations were low. The concentration of 6 He–V clusters, however, increased significantly with increasing irradiation time near the incident surface in a region from 0.05 μm to 1 μm thick. The formation of these clusters is an important factor that influences the mechanical properties of material.

3.2. Damage accumulation at the divertor surface

The effects of a low energy, high flux helium plasma on the formation of helium–vacancy clusters were studied. Fig. 3 shows the time and depth dependence of helium concentration in neutron unirradiated (a) and neutron irradiated tungsten (b) at 873 K, where the incident helium energy was 30 eV, and the flux was $10^{22}/m^2s$. In this condition the helium was distributed widely in the specimen due to rapid diffusion, and the distribution of helium reached steady state at 1 s. The concentration of helium was about 10^{-8} except near the back surface. This value was only about three hundred times higher than that of high energy, low flux helium described in Section 3.1, although the helium flux was four orders of magnitude higher in the present case. The ratio of helium that escaped from the incident surface to that which diffused into the matrix is determined by the depth of

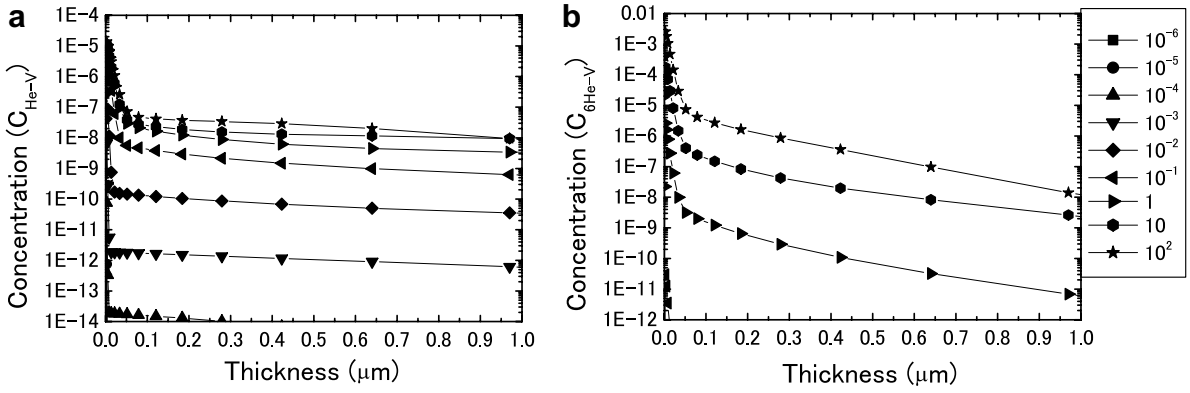

Fig. 2. Time and depth dependence of formation of the helium–vacancy clusters He–V (a) and 6 He–V (b) under helium irradiation with energy of 1 keV and flux of $10^{18}/m^2s$ and neutron irradiation at 873 K. Irradiation times for each curve, in seconds, are shown in the insert legend.

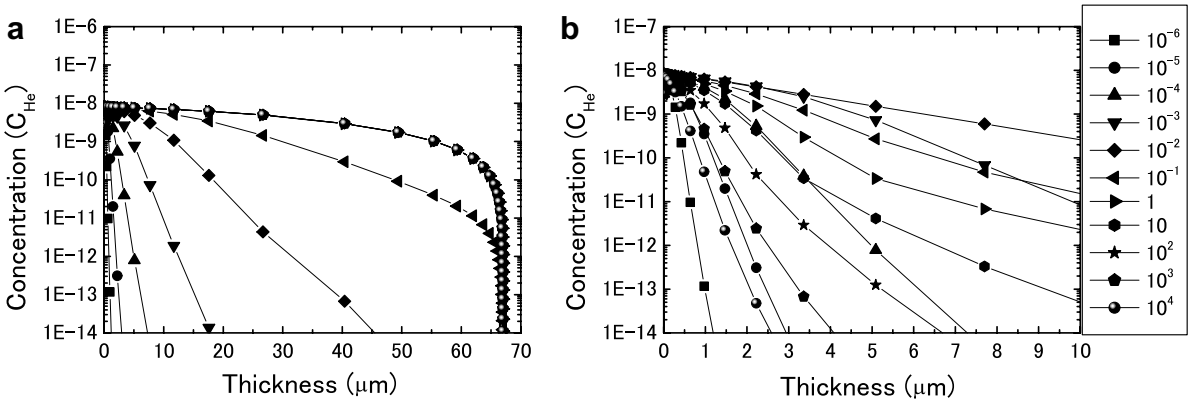

Fig. 3. Time and depth dependence of helium concentration with energy of 30 eV and flux of $10^{22}/m^2s$ in neutron unirradiated (a) and neutron irradiated (b) tungsten at 873 K. Irradiation times for each curve, in seconds, are shown in the insert legend.

injected helium, which depends on the incident energy. In the present study, the centers of helium distribution peaks were 0.2 nm and 2 nm for 30 eV case and 1 keV case, respectively. The fraction of helium that diffused into the matrix was 3×10^{-7} in the former and 2.8×10^{-5} in the latter case. In neutron irradiated tungsten, vacancies formed by the neutron displacement damage modified the diffusion and accumulation of the helium, the same as in the case shown in Fig. 1(b).

Fig. 4 shows the time evolution of the depth distribution of He–V (a) and 6 He–V (b) clusters. The concentration of He–V clusters increased with increasing irradiation time to 1 s, and then continued to increase near the incident surface, but began to decrease in the deeper regions of the specimen. The peak concentration of He–V clusters shifted toward the incident surface with increasing irradiation time after 1 s. After irradiation for 100 s, the concentration of 6 He–V clusters in a 3.5 μm wide zone near the incident surface increased, and saturated in the region deeper than 3.5 μm with increasing irradiation time. The peak concentration of 6 He–V clusters was 10^{-2} after irradiation of 10^4 s, which was equal to the concentration of vacancies produced by the neutron irradiation. This means that all vacancies trapped helium to form 6 He–V clusters. Compared with the formation of 6 He–V clusters induced by helium with energy of 1 keV as shown in Fig. 2, where the irradiation time was 100 s, the concentration of helium–vacancy clusters near the incident surface was low for the same irradiation time, and the width of the concentration peak of 6 He–V clusters

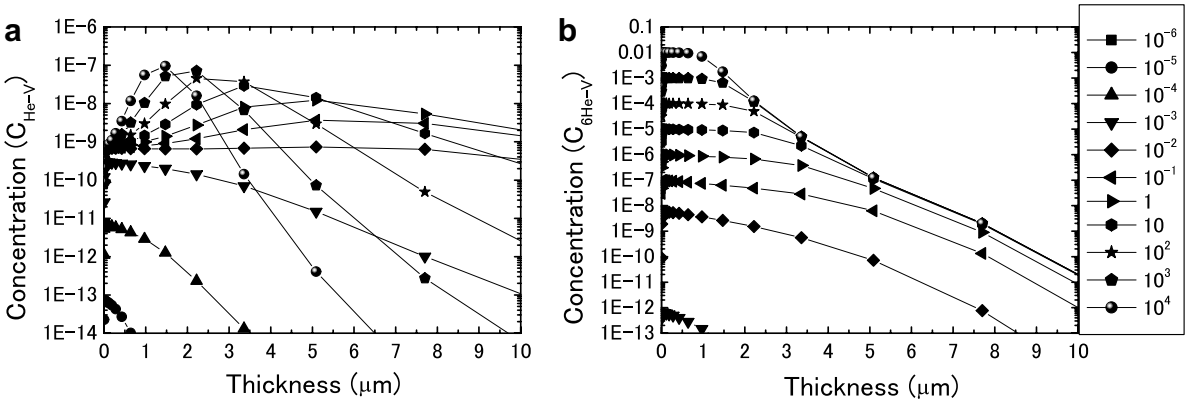

Fig. 4. Time and depth dependence of formation of the helium–vacancy clusters He–V (a) and 6 He–V (b) under helium irradiation with energy of 30 eV and flux of $10^{22}/m^2s$ and neutron irradiation at 873 K. Irradiation times for each curve, in seconds, are shown in the insert legend.

was larger in the case of 30 eV helium. The low production rate of vacancy in the latter case decreased the trapping of helium to form helium–vacancy clusters, and resulted in helium diffusion deeper into the specimen. It is clear that the diffusion of helium is easy in the case of low energy, high flux helium. It suggests that the surface damage caused by the formation of helium–vacancy clusters near the incident surface is more prominent in the divertor than in the first wall.

4. Conclusions

Synergistic effects of helium plasma bombardment on the microstructural evolution induced by neutron irradiation in tungsten were studied by computer simulations based on the rate theory considering diffusion and reaction of helium and defects. Vacancies formed by the neutron irradiation trap helium to form helium–vacancy clusters. Prominent accumulation of the helium–vacancy clusters spreads widely within a few μm of the incident surface. Formation of the clusters will change neutron irradiation effects, such as blistering, void swelling and irradiation hardening. Understanding these synergistic effects of helium plasma and neutron irradiation is important for the estimation of damage to the PFMs.

References

[1] S.K. Das, M. Kaminsky, in: M. Kaminsky (Ed.), Advanced in Chemistry Series, vol. 158, American Chemical Society, Washington, DC, 1976, p. 112.
[2] N. Yoshida, H. Iwakiri, K. Tokunaga, T. Baba, J. Nucl. Mater. 337–339 (2005) 946.
[3] H. Iwakiri, Doctor Dissertation, Kyushu University, 2004.
[4] K. Tokugana, O. Yoshikawa, M. Makise, N. Yoshida, J. Nucl. Mater. 307–311 (2002) 130.
[5] P. Klaver, E. Haddeman, B. Thijsse, Nucl. Instrum. and Meth. B 153 (1999) 228.
[6] W.D. Wilson, R.A. Johnson, in: P.C. Gehlen, J.R. Beeler, R.I. Jaffee (Eds.), Interatomic Potentials and Simulation of Lattice Defects, Plenum, New York, 1972, p. 375.
[7] Q. Xu, N. Yoshida, T. Yoshiie, Mater. Trans. 46 (2005) 1255.
[8] G. Federici, J.N. Brooks, D.P. Coster, G. Janeschitz, A. Kukushkin, A. Loarte, H.D. Pacher, J. Stober, C.H. Wu, J. Nucl. Mater. 290–293 (2001) 260.
[9] J.P. Biersack, L.G. Haggmark, Nucl. Instrum. and Meth. 174 (1980) 257.
[10] Q. Xu, T. Yoshiie, H.C. Huang, Nucl. Instrum. and Meth. B 206 (2003) 123.
[11] T. Yoshiie, X. Xu, Q. Xu, S. Yanagita, Y. Satoh, ASTM STP 1398, 2001, p. 625.
[12] L.M. Caspers, H. Van Dam, A. Van Veen, Delft. Progr. Rep. Ser. A 1 (1974) 39.
[13] S. Fukuzimi, T. Yoshiie, Y. Satoh, Q. Xu, H. Mori, M. Kawai, J. Nucl. Mater. 343 (2005) 308.
[14] F. Dausinger, Philos. Mag. A37 (1978) 819.
[15] J.Th.M. de Hosson, A.W. Sleeswyk, L.M. Caspers, W. van Hengten, A. van Veen, Solid State Commun. 18 (1976) 479.